2
Experimental and Analytical Techniques

The role of appropriate experimental and analytical procedures is vital in accomplishing the desired goals of device exploration. Selection of an appropriate experimental method depends on several factors like cost, performance and fabrication suitability. During and after device fabrication, appropriate material and electrical characterizations are required. Accurate data obtained by correct parameter extraction techniques enable to draw definite conclusions on the science behind the phenomenon. In this chapter, a brief overview is presented on the major experimental, characterization and parameter extraction techniques used in the present research work.

2.1 ATOMIC LAYER DEPOSITION

Atomic layer deposition (ALD), is a thin film technology conceptually based on chemical vapor deposition (CVD) method [George, 2010]. Various types of materials including oxides, nitrides, carbides, metals, sulphides, fluorides, biomaterials and polymers can be deposited using ALD [Beneq, 2005]. In addition, doping and growth of nano-laminates and mixed structures can also be performed using ALD [Beneq, 2005].

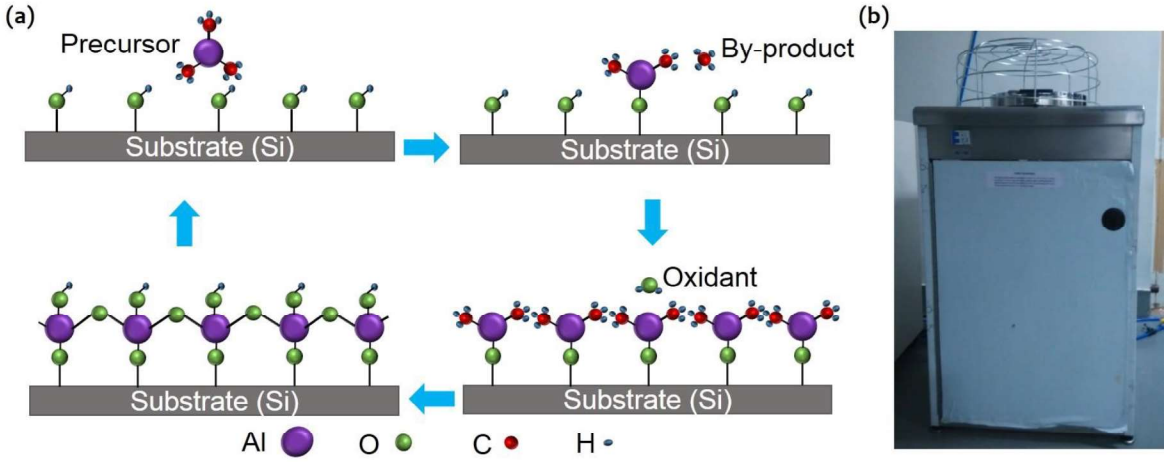

Figure 2.1: (a) A complete cycle in the atomic layer deposition process. **(b)** Savannah S-200 ALD system from Cambridge nanotech used in experiments.

In principles, it is a surface controlled thin film deposition technique where an inert carrier gas flowing through the system injects very short pulses of the vapors of gaseous precursors in the reaction chamber. The film growth takes place in a repetitive style. In the most general case, there are four steps in one cycle: (i) exposure of the first precursor, (ii) purging or evacuation of first precursor from the reaction chamber, (iii) exposure of the second precursor, and (iv) purging or evacuation of second precursor from the reaction chamber. When a surface terminated with functional groups is exposed to the precursor, its molecules react with these groups of surface releasing byproducts. The subsequent purge step evacuates all the excess

precursor molecules and volatile byproducts leaving only the monolayer on the surface. Successively, the other precursor is infused in the chamber and reacts with the chemisorption layer liberating the byproducts and producing the desired film. Simultaneously, the surface attains its original state. The second purge step concludes a single deposition cycle. This process is repeated several times to get the desired film thickness [George, 2010, Johnson *et al.*, 2014]. The presence or the absence of reactive functional groups like hydroxyl groups on the surface of the growing film determines the chemical reactions taking place in the chamber under each exposure cycle [Ritala and Leskela, 2002]. Its advantages include precise film thickness control, defect free films, conformal coating of large–area substrates and complex 3D features and a high repeatability and scalability.

In the current study, savannah S-200 thermal ALD system from Cambridge nanotech was used to deposited thin layers of inorganic dielectric HfO_2 using tetrakis-dimethyl-amidohafnium (TDMAH) and water as the precursors. Keeping the maximum operational temperature with the flexible substrates under consideration, the deposition was performed at 100 °C. A basic operating cycle of an ALD process and image of the system is shown in Figure 2.1.

2.2 SPIN COATING

Spin coating is one of the widely used techniques for depositing thin films from the solutions on the substrates. The process of spin coating generally involves the formation of a thin film with thickness varying from a few nanometers to a few microns uniformly on the substrate by dispensing the solution of the desired material in the solvent and rotating it on high speeds varying from 200 to 4000 rpm [Birnie, 2004, Hall *et al.*, 1998]. In spin coating, a solution of the material to be deposited is made in a volatile solvent by mixing the material and the solvent and stirring for few hours. This solution is dispensed on the substrate and substrate is rotated at high speeds. The rotation of the substrate and the solution enables uniform spreading of the adequate amount of the solution and spilling of the excess solution off the substrate. A rapid air-flow dries the majority of the solvent and provides uniformity to the deposited layer while leaving just the molecules of the material on the substrate [Ossila, 2017]. Thickness of the final film of the material depends on several factors of the solution (solvent boiling point, solution viscosity, material solubility in the solvent, material concentration in the solution) and spinning conditions (spin speed, time, acceleration and position) [Birnie, 2004]. The main advantages of spin coating include quick and easy production of highly uniform films. The main demerit is the very fast drying time, which sometimes may result into a lower performing device due to unavailability of time for molecular arrangement.

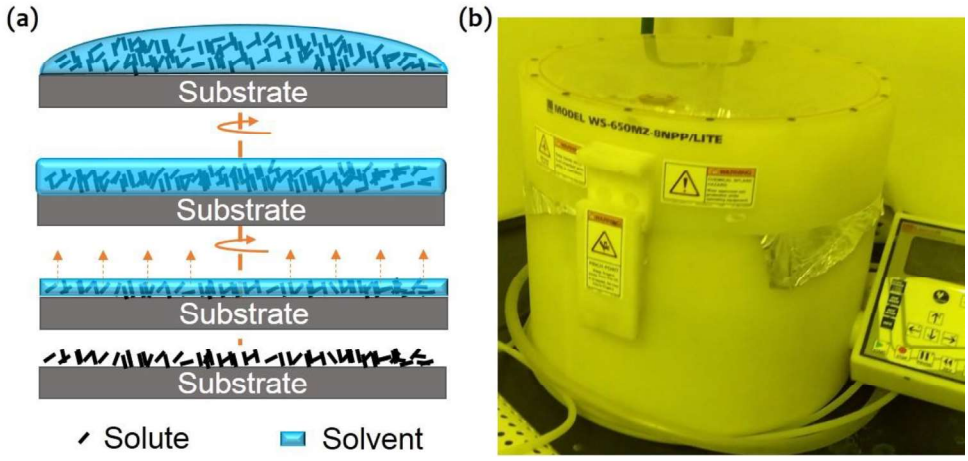

Figure 2.2: (a) Complete process of film formation in spin coating method. **(b)** WS-650 MHz-BNPP/LITE spin coating system from Laurell used in experiments.

Keeping the above issues under consideration in the current study, spin coating has only been used to deposit the polymeric insulator layer. Spin coatings were performed using WS-650 MHz-BNPP/LITE spin coating system from Laurell. The spin speed used varied from 1500-2000 rpm with a fixed spin time of 30 s. Depending on the type of the substrate being used (flexible or rigid), a post-deposition annealing was also performed at 100 °C or 150 °C. The schematic of the spin process and digital image of the spin coater used is shown in Figure 2.2.

2.3 DROP CAST

Drop cast is the most trivial method of thin film deposition from liquid solutions. In this procedure the solution is simply poured over the substrate. An eventual solvent evaporation from the dispensed solution leads to formation of thin film of the solute on the substrate [Chávez *et al.*, 2013, Park *et al.*, 2006], which is schematically illustrated in Figure 2.3(a). Rate of film formation depends on the rate of solvent evaporation which in turn depends on the boiling point of the solvent used. In general, relatively thick films are obtained from this scheme. General advantages of this scheme include simplicity, low material consumption and no-equipment-needed nature. However there are some demerits of this scheme like non-uniformity and uncontrolled film nucleation and growth. In the current study, the active organic semiconductor layer has been deposited by this scheme. Main purpose to use this scheme was to exploit the benefit of slower rate of film formation. A decelerated rate of film formation provides more time for molecular settlement and hence a higher degree of crystallinity [Bi *et al.*, 2015]. In the current study, rate of solvent evaporation was further reduced by covering the sample carrying the solution from a petri dish, which created a solvent rich environment in the covered area, leading to a very slow rate of solvent evaporation. Figure 2.3(b) shows an actual image of a drop casted sample, whereas the final film/crystals formed are shown in Figure 2.3(c).

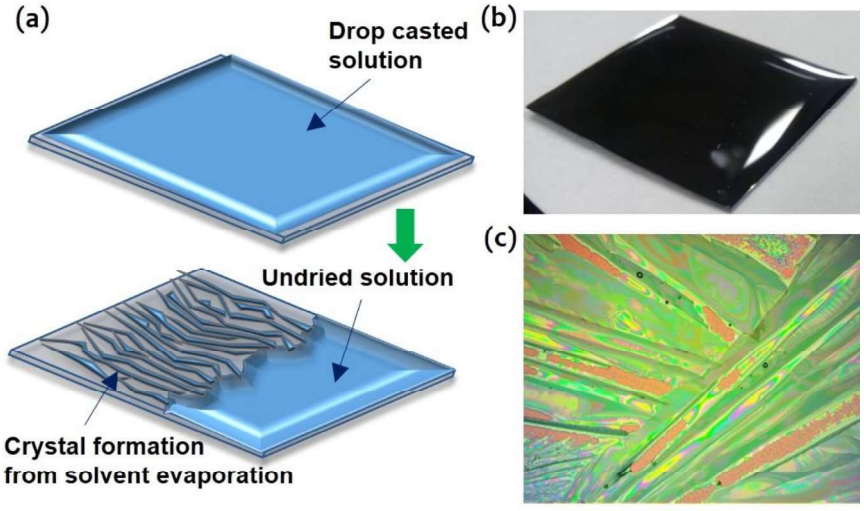

Figure 2.3: (a) Drop casting procedure and crystal formation. **(b)** Actual drop casting on a silicon sample. **(c)** Optical micrograph of obtained crystals.

2.4 THERMAL EVAPORATION

Thermal evaporation is one of the very popular physical vapor deposition scheme. This process involves heating the material to be deposited, transport of the vapors of the material from source to target and condensation of the vapors on the substrate in the form of a thin film [Kern, 2012, Mattox, 2010]. Material to be deposited is resistively heated in a tungsten boat. In most of the systems, the boat is installed at the bottom of the chamber to avoid spilling of the liquefied material, whereas the target substrates are mounted on the ceiling of the chamber. For resistive heating of the materials, very high levels of vacuum (> 10^{-6} Torr) are required. Due to

high vacuum in the deposition chamber, molecules of the material (vapors) can travel a longer distance before getting scattered from gas molecules. In other words, the mean free path of the vapors is increased and vapors can easily reach on the target substrate. At vacuum levels higher than 10^{-5} Torr, mean free path is longer than a few meters, which means that vapors can travel directionally in a straight line from source to target. Further, high vacuum levels are also desired in order to achieve high purity of the deposited films. Presence of small amount of oxygen may be detrimental for the film quality, hence pumping out all the gases at vacuum level higher than 10^{-6} Torr greatly improves the purity of the film [Semicore Engineering, 2017, Hardy, 2013]. After reaching the target (i.e. the cold substrate), vapors molecules condense in the form of a thin film. Figure 2.4(a) shows the schematic illustration of the thermal evaporation process. In the current study, thin metallic layers of gold (Au) were deposited by vacuum evaporation using SC-Triaxis-e-beam and thermal evaporation system from Semicore shown in Figure 2.4(b). All depositions were carried out at a vacuum level of 10^{-6} Torr and with a deposition rate of 1 Å/s. Source material of Au was heated in tungsten boat at power of 600 W. Source to target distance was 20-60 cm. In-situ film thickness monitoring was done using quartz crystal based oscillator. Final thickness of Au film was 200 nm which was further verified using stylus based profilometer measurement.

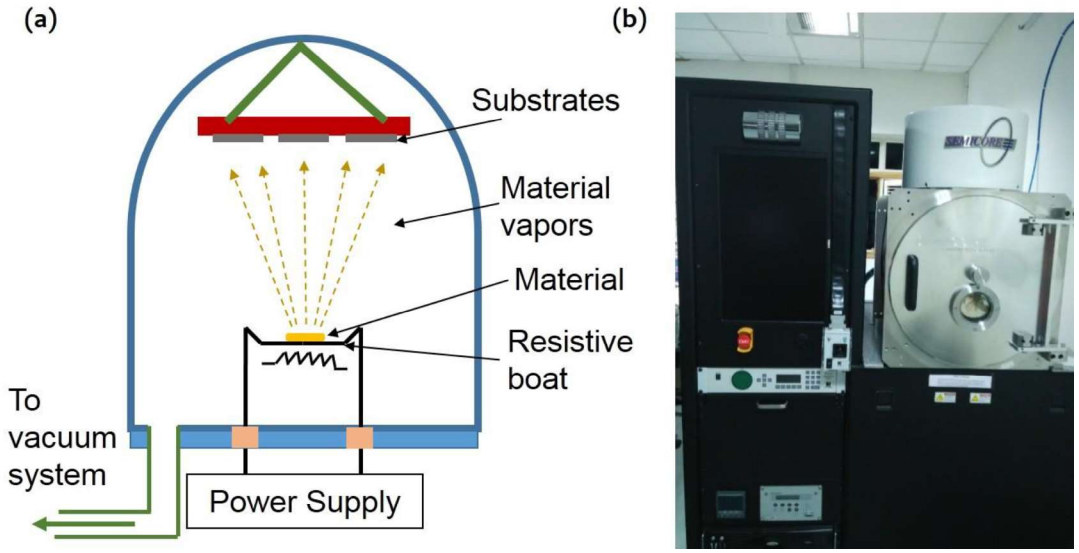

Figure 2.4: (a) Material deposition in thermal evaporation method. **(b)** SC-Triaxis thermal evaporation system from Semicore used in experiments.

2.5 SURFACE PROFILING

Linear surface profiles of various surfaces can be traced using a surface profiler. Surface profiling is one of the most easy and apt technique to measure the profile of a surface [Dong-Hyeok and Nahm-Gyoo, 2012]. Surface profiling involves scanning of the line of the interest with a stylus [Whitehead *et al.*, 1999]. Stylus is a probe with a very sharp tip. The vertical stage of the profiler which carries the stylus, mechanically moves in upward and downward direction depending on the surface feature. During scanning, stylus exerts a very small amount of constant mechanical force on the surface. A closed feedback loop monitors and maintains the value of this constant force as the stylus moves along the features of the surface. The change in the z position of the stage carrying the stylus is recorded and used to construct the profile of the surface [Nanoscience Instruments, 2017]. Figure 2.5(a) depicts the process of the surface profile measurement. Since the stylus is in contact of the surface to be scanned, it is highly sensitive and accurate. The resolution and accuracy of the measurements also depends on scan time, sharpness of the stylus probe tip. The main disadvantage of the stylus based profilometry is that it can be destructive for some surfaces and tip of the stylus can be contaminated by some surfaces which can lead to erroneous results. In the current study, linear surface profiling and

various thickness measurements were performed using DekTak-XT surface profiler from Bruker, which is shown in Figure 2.5(b). The radius of the stylus used was 2 μm and scan time was 30 s to 60 s.

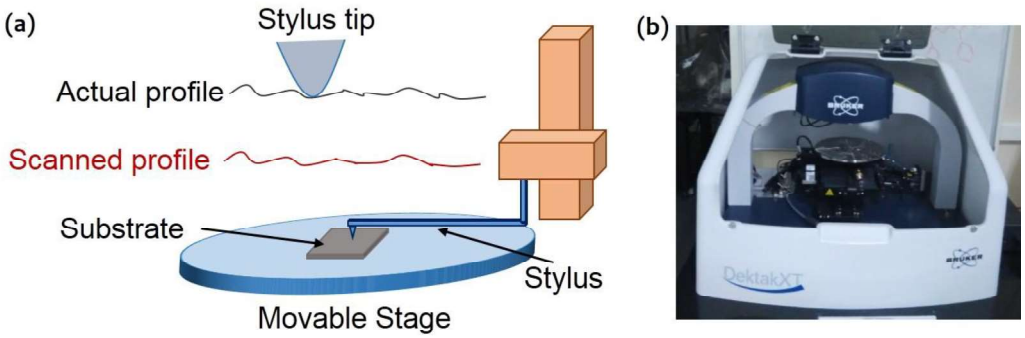

Figure 2.5: (a) Linear surface profile measurement from stylus based profilo-meter. **(b)** DektakXT surface profilo-meter system from Bruker used in measurements.

2.6 X-RAY DIFFRACTION

X-ray diffraction studies are among the fundamental analytical techniques which are primarily used for phase detection in crystalline materials, to determine unit cell dimensions, and to estimate the particulate sizes in the substance [Ewald, 1962]. XRD measurements involve generation of X-rays, their bombardment on the materials and detecting the reflected X-rays. An X-ray diffractometer has three parts; X-ray tube, sample holder and a detector. X-rays are produced in a cathode ray tube, where a high voltage is applied across the filament. Electrons are emitted by the heated filament, which are accelerated towards the target material. The characteristic X-ray spectra of the target material are generated, when the bombarding electrons have sufficient energy to remove the inner shell electrons of the target material. There are many components in the emission spectra, where the most common are K_α (transition from n = 2 to n = 1) and K_β (transition from n = 3 to n = 1). Different K_α wavelengths are typical of the target material (Cu, Fe, Mo, and Cr). Monochromatic X-rays are further produced by filtering the K_α from the characteristic emission spectra. These monochromatic X-rays are collimated and directed towards the material to be analyzed. The intensity of the reflected X-rays is recorded by a rotating detector. A detector records and processes this X-ray signal and converts the signal to a count rate which is then output to a device such as a printer or computer monitor [Dutrow and Clark, 2016]. When the incident X-rays on the material satisfies the Bragg's Equation, $n\lambda = 2dsin\theta$, a constructive interference and a peak in intensity is observed [Elton and Jackson, 1966]. In the current study, X-ray diffraction measurements were performed using D8 advanced from Bruker, which uses Copper as the target material with CuK_α radiation = 1.5418Å. Figure 2.6 shows the basic illustration of the Bragg's law and digital image of the X-ray diffractometer.

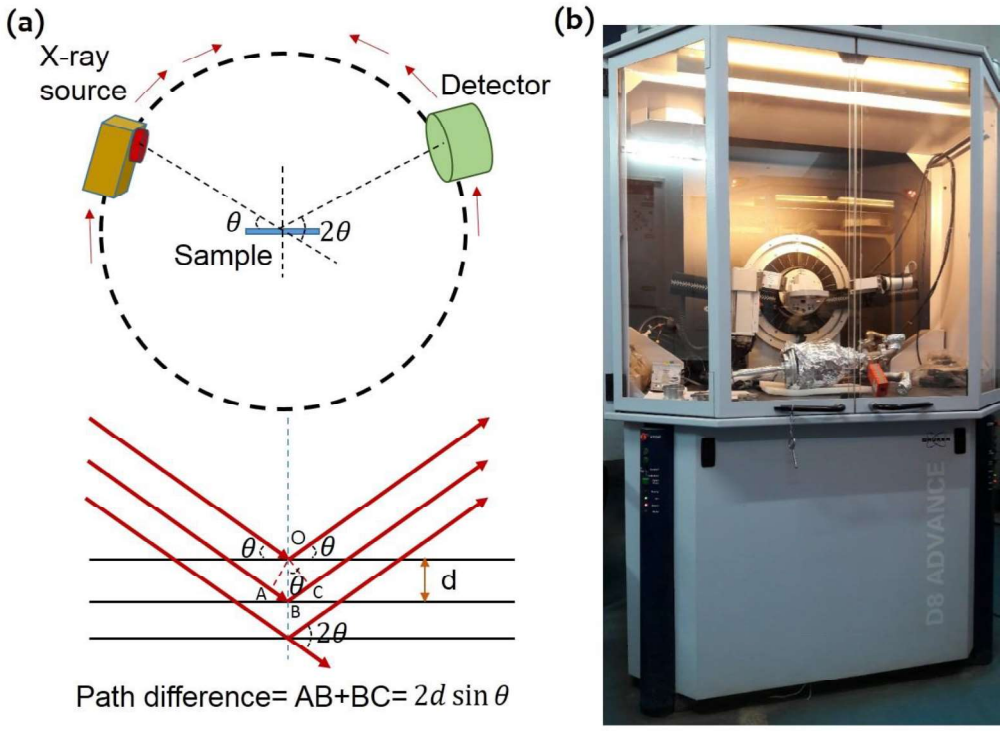

Figure 2.6: (a) Simplified principle of X-ray diffraction measurements. **(b)** D8-advanced X-ray diffraction measurement system from Bruker used in analysis.

2.7 ATOMIC FORCE MICROSCOPY

Atomic force microscopy (AFM) is certainly one of the most advanced microscopy technology for analysing the surfaces at nano-scale. This microscopy technology not only images the three dimensional morphology, but it also provides various types of parameters related to surface characteristics [Haugstad, 2012]. In principle, a cantilever with a very sharp tip is used to scan over the sample surface. As the tip reaches very close to the surface, the attractive forces between the surface and the tip become active and the cantilever deflects towards the surface. However, when the tip moves even closer to the surface, repulsive forces become dominant and cause the cantilever to deflect away from the surface. The cantilever deflections are detected by a laser beam. This laser beam is reflected off the flat top of the cantilever. Any change in the direction of reflected beam will be tracked by a position-sensitive photo diode (PSPD). An AFM image of a sample surface is generated by scanning the cantilever over an area of interest. The features on the sample surface cause deflections in the cantilever, which in turn change the direction of reflected beam and are recorded by the PSPD. A constant tip height over the sample surface is maintained by a feedback loop [Park Systems, 2017]. Atomic force microscopy in the current study was performed using SPM XE-70 from Park Systems. A simplified operating principle of the atomic force microscopy technique and AFM instrument used in the current study are shown in Figure 2.7.

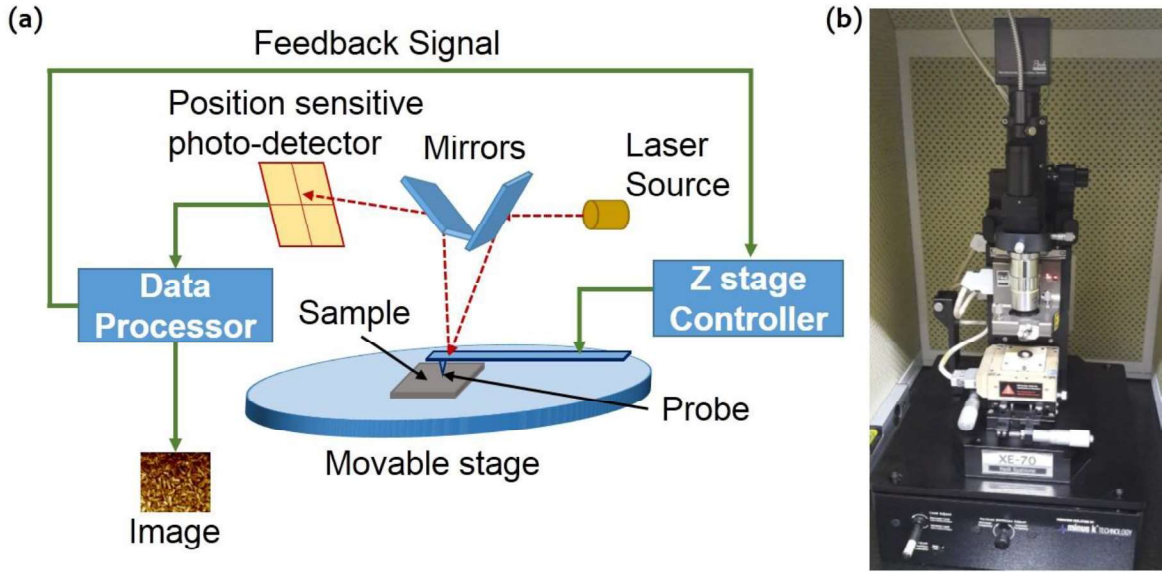

Figure 2.7: (a) Simplified working principle of atomic force microscopy technique. **(b)** XE-70 surface probe microscopy system from Park Systems used in surface characterization.

2.8 SCANNING ELECTRON MICROSCOPY

Scanning electron microscopy (SEM) is one of the widely used microscopy technology for imaging micro and nano-scale surface morphology of solid samples. It involves the interaction of a focused beam of high energy electrons and sample surface which reveals the morphology. Small surface areas can be imaged at very high magnification ranging from 20× to 30,000× in the spatial resolution of 50-100 nm [Egerton, 2005, Reimer, 1998]. The main SEM components include a source of electrons, a vertical zone with electromagnetic lenses through which electrons can travel down to sample surface, an electron detector, a chamber for placing samples and a computer to control and display the microscopy. The vertical column and the chamber are evacuated by vacuum pumps. Electrons are emitted from the top of the vertical column and accelerated down. These electron bunches become a focus beam of electron after passing through several lenses and apertures, which collides with the sample surface. The position of the electron beam on the sample can be controlled by scan coils situated above the objective lens. A variety of signals are generated from the interaction of energetic beam of electrons and samples which include secondary electrons, backscattered electrons, diffracted backscattered electrons, photons, visible light, and heat. Secondary electrons are used to produce the sample images. Diffracted backscattered electrons have applications in determining the crystal structures and photons are used for elemental analysis. Role of secondary electrons is the most important for showing morphology and topography of the sample surfaces and backscattered electrons are helpful for illustrating contrasts in samples [Nanoscience Instruments, 2017, Swapp, 2016]. SEM in the current study was performed using EVO-18 special edition from Carl-Zeiss. A simplified operating principle of the scanning electron microscopy and SEM instrument used in the current study are shown in Figure 2.8.

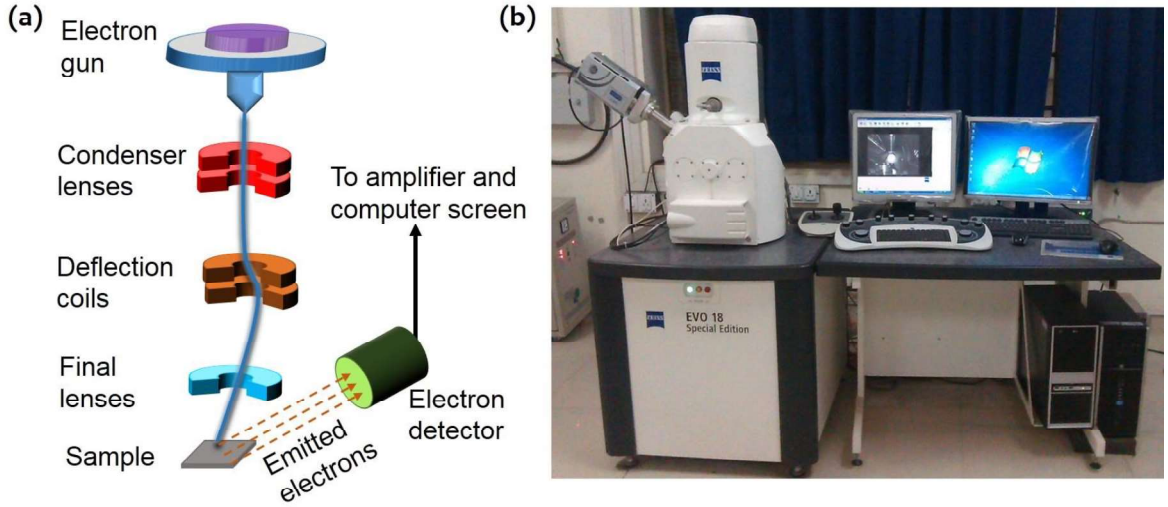

Figure 2.8: (a) Simplified working principle of scanning electron microscopy. **(b)** EVO-18 special edition scanning electron microscope from Carl Zeiss used in characterization.

2.9 ULTRA-VIOLET AND VISIBLE ABSORPTION SPECTROSCOPY

Ultra-violet and visible spectroscopy is one of the important analysis techniques in analytical chemistry. It is used to analyze the interaction between light and matter in the wavelength range of 200 nm to 800 nm [Perkampus, 1992]. Working principle is based on the absorption of the optical energy by the chemical substances when electrons make transition from lower energy level to higher. UV-visible spectroscopy obeys Beer-Lambert's law, according to which the absorbance depends on intensity of incident radiation, thickness of the absorbing solution and concentration of the solution [Swinehart, 1962]. Most of the modern UV-visible spectrophotometers have light sources to emit radiation in UV and visible region of the electromagnetic spectrum. The emitted light is dispersed in the form of increasing monochromatic wavelengths with the help of rotating prisms. Each wavelength is selected with the help of slits and is further separated into two beams with the help of another prism. These two beams are passed from sample and reference solutions contained in quartz cuvettes. Two photocells monitor the intensity of light coming out from the reference and sample solutions, which induces alternating currents in the photocell. These current signals are passed to an amplifier, which convert these signals into absorbance [Thakur, 2011, Yalamarthy, 2013]. In the current study, UV-visible spectroscopy was performed in wavelength range of 250-800 nm using UV1800 spectrophotometer from Shimadzu. Figure 2.9 shows the simplified working principle and image of the UV-visible spectrophotometer used in the study.

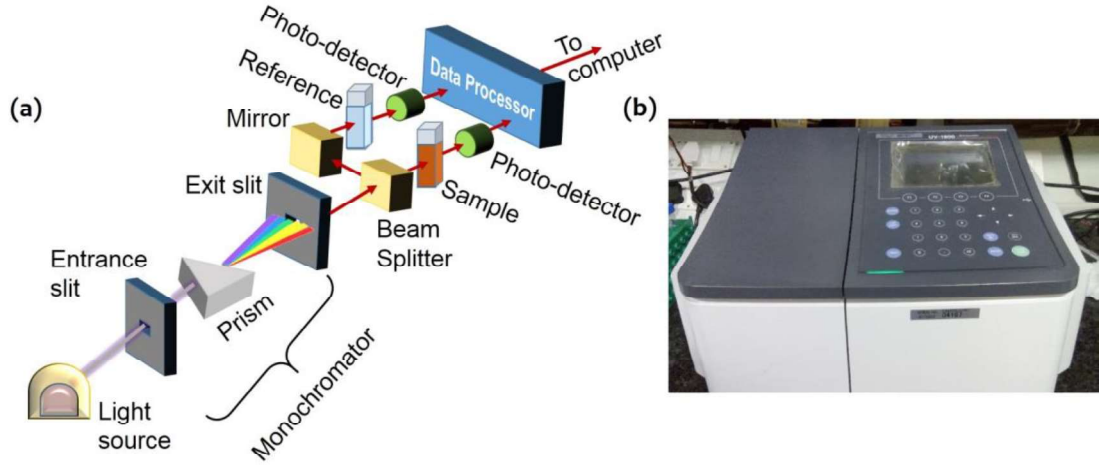

Figure 2.9: (a) Simplified working principle of UV-visible absorbance spectroscopy. **(b)** UV-1800 UV-visible spectrophotometer from Shimadzu used in characterization.

2.10 ELECTRICAL CHARACTERIZATION

Electrical characterization of the fabricated devices was performed using 4200-semiconductor characterization system (SCS) from Keithley which is a modular and fully integrated parameter analyser capable of executing current-voltage (I-V) and capacitance-voltage (C-V) characterization [Tektronix, 2017]. In the current study, characterizations were performed with the help of Keithley interactive test environment (KITE). All the measurements were performed with device positioned on Cascade Microtech PM5 probe station in dark and ambient conditions. Device under test on the probe station was connected to source measuring units (SMUs) of the parameter analyser through triax coaxial cables. Figure 2.10 shows the image of 4200-SCS and the probe station used in the current study for device characterization.

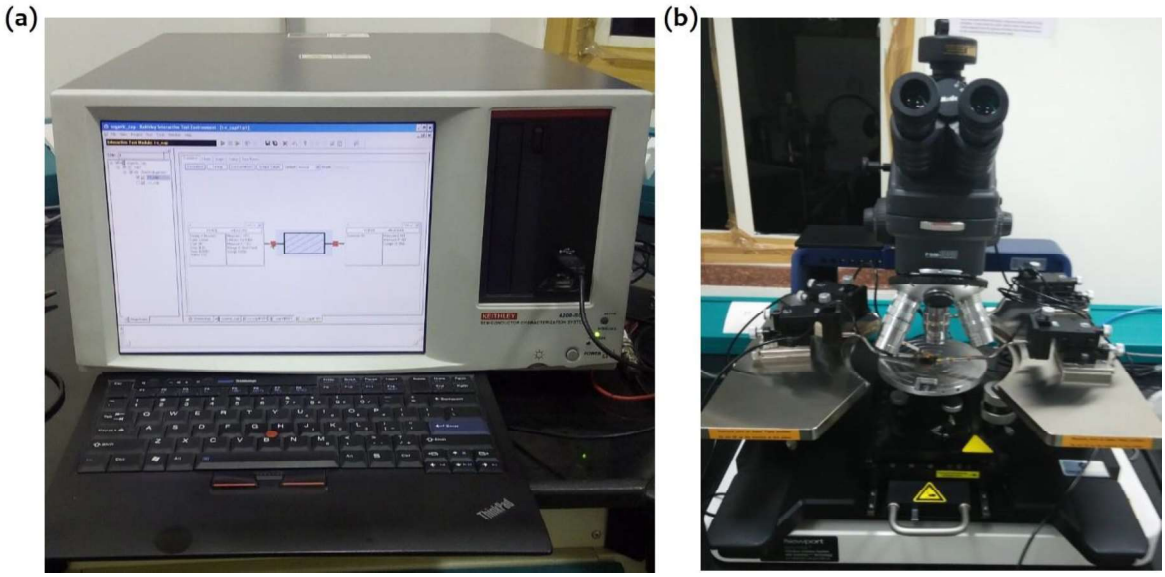

Figure 2.10: (a) 4200-SCS Semiconductor parameter analyzer from Keithley used in electrical characterization. **(b)** PM-5 probe station from Cascade Microtech used for housing and probing sample during electrical characterization.

2.11 PARAMETER EXTRACTION

The superiority of a device can be determined from its characteristics parameters. Characteristics parameters of a device depend on several material and process based factors which critically affects performance of the device [Meller and Grasser, 2009]. OFETs are also evaluated for their performance with many characteristic parameters. The main OFET device parameters include field-effect mobility (μ), threshold voltage (V_{TH}), on-off ratio (I_{ON}/I_{OFF}), sub-threshold slope (SS), and interface trap density (D_{it}) [Li, 2011]. All of these parameters depend on numerous material factors (type of organic semiconductor, insulator and electrode materials) and process factors (deposition method of organic semiconductor and insulator, deposition parameters, environmental conditions). All the factors above strongly influence the characteristic parameters.

To extract these parameters, variation in the drain current (I_{DS}) is plotted with applied gate (V_{GS}) and drain bias (V_{DS}). The electrical characteristic, which plots I_{DS} vs. V_{GS} is known as the transfer characteristics of the OFET. Similarly, the plot of I_{DS} vs. V_{DS} is known as the output characteristics [Sun and Dalton, 2008]. A sample transfer and output characteristics of a p-channel OFET is shown in Figure 2.11.

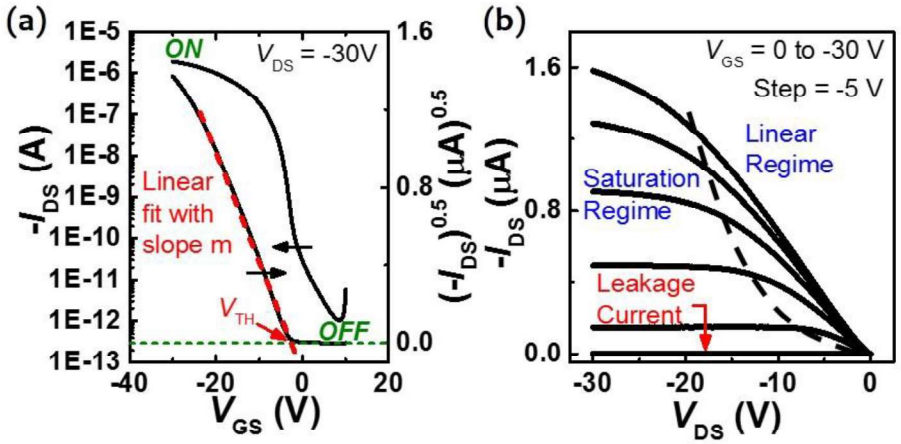

Figure 2.11: A transfer **(a)**, and output **(b)** characteristics of a specimen OFET, showing various electrical parameters of the device.

At positive value of gate bias, due to absence of holes, only very small leakage current flows, and the transistor remains in OFF state. However, as the gate bias takes negative values, holes begin to accumulate in the semiconductor layer near the dielectric-semiconductor interface. After a certain offset gate bias, when substantial hole accumulation has occurred, the conduction between source and drain terminals commences. The drain current rises sharply and transistor is turned ON. Device can operate either in the linear (at low $|V_{DS}|$) or in the saturation regime (at high $|V_{DS}|$). The dotted line in the output characteristics separates out the linear and saturation regime of the transistor operation. The drain current in the linear mode of operation can be given as following,

$$I_{DS} = \mu C_{ox} \frac{W}{L}\left[(V_{GS} - V_{TH})V_{DS} - \frac{V_{DS}^2}{2}\right] \qquad (2.1)$$

Where μ is the field-effect mobility, C_{ox} is the capacitance density, V_{TH} is threshold voltage of the device and W and L are channel width and length respectively [Klauk, 2006]. In the saturation regime, drain current can be given as,

$$I_{DS} = \mu C_{ox} \frac{W}{L}\frac{(V_{GS} - V_{TH})^2}{2} \qquad (2.2)$$

Most of the transistor parameters can be extracted from the transfer characteristics of the device. The most important parameter of field-effect mobility which is a measure of the ease with which charge carriers can flow in a semiconductor, can be extracted from the transfer characteristics by plotting square root of drain current vs. gate voltage. The slope of square root of drain current can be extracted by applying a linear fit in the above curve [Klauk, 2006]. The slope of the square root of drain current can be defined mathematically as,

$$m = \frac{\partial\sqrt{I_{DS}}}{\partial V_{GS}} \qquad (2.3)$$

For $V_{GS} > V_{TH}$, derivative of equation (2.2) can be rewritten as following,

$$\mu = \frac{2L}{WC_{ox}}\left(\frac{\partial\sqrt{I_{DS}}}{\partial V_{GS}}\right)^2 = \frac{2L}{WC_{ox}}m^2 \qquad (2.4)$$

Above equation is the most standard analytical way for mobility extraction. Another parameter, the threshold voltage (V_{TH}) can be defined as the minimum offset voltage required for conduction to take place [Klauk, 2006]. V_{TH} can also be extracted from the above linear fit applied on the square root of drain current. V_{TH} of the device can be obtained as the negative ratio of intercept and the slope of the linear fit. The current on-off ratio (I_{ON}/I_{OFF}) can be defined as the ratio of the drain currents in the ON and OFF state respectively [Klauk, 2006]. In the

current study, the maximum value of the drain current has been taken as I_{ON} and minimum constant level in the OFF state has been considered as I_{OFF}. In some cases, where the drain current is not constant in the off state, the minimum level of the drain current has been assumed as the I_{OFF}. The subthreshold slope (SS) is related with the switching speed of transistors [Qin *et al.*, 2006]. A transistor with steeper slope shows faster transition between ON and OFF states. The SS can be obtained from the transfer characteristics by determining the minimum difference in V_{GS} in which I_D changes by 10 times. D_{it} is another parameter providing the density of interfacial trap state and thus a measure of the quality of the dielectric-semiconductor interface. It can be directly calculated from SS using following equation,

$$D_{it} = \frac{C_i}{q}\left[SS \frac{\log(e)}{kT/q} - 1 \right] \tag{2.5}$$

Where q is the electron charge, e is the base of the natural logarithm, k is the Boltzmann's constant, and T is the temperature in Kelvin [Held *et al.*, 2015].

…